Title	Figure-of-merit enhancement of surface plasmon resonance sensors in the spectral interrogation
Author(s)	Shalabney, A.; Abdulhalim, Ibrahim
Citation	Shalabney, A.,& Abdulhalim, I. (2012). Figure-of-merit enhancement of surface plasmon resonance sensors in the spectral interrogation. Optics Letters, 37(7), 1175-1177.
Date	2012
URL	http://hdl.handle.net/10220/18693
Rights	© 2012 Optical Society of America. This paper was published in Optics Letters and is made available as an electronic reprint (preprint) with permission of Optical Society of America. The paper can be found at the following official DOI: [http://dx.doi.org/10.1364/OL.37.001175]. One print or electronic copy may be made for personal use only. Systematic or multiple reproduction, distribution to multiple locations via electronic or other means, duplication of any material in this paper for a fee or for commercial purposes, or modification of the content of the paper is prohibited and is subject to penalties under law.

Figure-of-merit enhancement of surface plasmon resonance sensors in the spectral interrogation

A. Shalabney[1,*] and I. Abdulhalim[1,2]

[1]Department of Electro-optic Engineering and the Ilse Katz Institute for Nanoscale Science and Technology,
Ben Gurion University of the Negev, Beer Sheva 84105, Israel

[2]School of Materials Science and Engineering, Nanyang Technological University 637722, Singapore
*Corresponding author: shalaban@bgu.ac.il

We show that adding a thin dielectric layer with high refractive index on top of the metallic layer in surface plasmon resonance sensors in the Kretschmann–Raether configuration in the spectral mode causes a redshift of the resonance wavelength, narrowing of the resonance dip, and an enhancement to the spectral sensitivity. Surprisingly, together with the sensitivity enhancement, the dip becomes much narrower and the figure of merit is considerably improved, particularly in the IR range. © 2012 Optical Society of America
OCIS codes: 240.6680, 240.6690, 280.4788.

Sensors based on surface plasmon resonance (SPR) in the Kretschmann–Raether (KR) configuration are attracting the interest of large group of researchers as well as industrial companies due to the high sensitivity and simplicity of this type of sensors. Detection limits on the order of pg/mm^2 are being reported using a variety of modes and detection techniques such as amplitude, angle resolved, wavelength resolved, and polarimetric and imaging approaches. Although SPR sensors exhibit the highest sensitivity among the sensors based on the evanescent-waves sensing principle, many researchers have attempted to improve their sensitivity and detection limit over the last decade [1]. In this aspect, many works were done on optimizing structural features such as modifying the prism refractive index (RI) [2,3], optimizing the metallic transducer layer [4], and using sculptured thin films instead of continuous metallic films [5,6]. Additional techniques were introduced using phase-sensitive SPR sensors [7,8] and fiber-optic-based configurations [9]. In our recent works [10,11] we have shown that the addition of a thin dielectric overlayer with high RI on the metal surface improves the angular sensitivity by nearly a factor of 3. However, one of the drawbacks of this modification is the broadening of the SPR dip by about factor of 3. Hence the figure of merit (FOM), which is defined as the ratio between the sensitivity S and the FWHM, did not change (FOM = S/FWHM). In this Letter we demonstrate both experimentally and theoretically that in the spectral mode the FOM is considerably improved due to simultaneous sensitivity enhancement and dip narrowing, particularly in the IR range.

When a thick enough dielectric layer is added on top of the metal surface it can support guided modes, and then the technique is called a guided-wave SPR (GWSPR) or coupled-wave SPR (CWSPR) sensor. In the GWSPR configuration, guided TM and TE modes evolve in addition to the SPR mode, and more than one dip can be observed in the reflectance in both the angular and spectral regimes [12]. Recently, these multiresonances were obtained also from chiral sculptured thin films and not only from homogenous dielectric layers [13]. When the thickness of the overlayer is below the cutoff thickness of the TM_0 guided mode, interesting implications on the sensor performances are realized. This case was suggested as a method for sensitivity enhancement by Lahav et al. [10,11]. In these works, the overlayer was a thin Si layer (~10 nm), and the major effect that was considered is the influence of this layer on the angular sensitivity of the sensor. Here we focus on the spectral interrogation mode, which is becoming more and more attractive due to the availability of miniature, cheap spectrometers and due to the importance in combining the SPR sensor with absorption spectroscopy for molecular recognition [14,15]. Following Lahav et al. [10,11] we call this configuration near-guided-wave SPR (NGWSPR) because the thickness of the overlayer dielectric film is below the cutoff for waveguided modes.

In order to prepare the NGWSPR structure, an Ag layer and thin Si overlayer were deposited on an SF11 glass slide substrate. The thicknesses of the Ag and the Si layers were planned to give optimal resonance response. The SF11 glass slide with the deposited layers was attached to the right-angle SF11 prism by a thin layer of index-matching fluid [Fig. 1(a)]. The entire assembly was mounted on an optical table with a 0.5° precision rotation stage in order to adjust the incidence angle inside the prism [see Fig. 1(a)]. As an analyte sample, a series of index-matching oils with RIs in the range of 1.31 to 1.35 in steps of 0.01 RI units (RIU) were used. The output of a halogen light source delivered using an optical fiber was collimated and P polarized. The reflected spectrum was collected by another objective and focused to the spectrometer through a 600 μm diameter core optical fiber. As a control sample, a thin Ag layer with no Si on it was deposited on SF11 glass and covered with a very thin thiol layer (~4 nm thickness) for protection. The control sample is used as the conventional SPR configuration.

In the first step, angular measurements were performed using both the SPR and the NGWSPR samples using a collimated 785 nm laser diode source. The incidence-angle resolution inside the prism is 0.28°. The angular measurements (not shown) were in particular performed to estimate the actual thicknesses of the layers and to plan the incidence angle for the spectral measurements. From the angular measurements, the
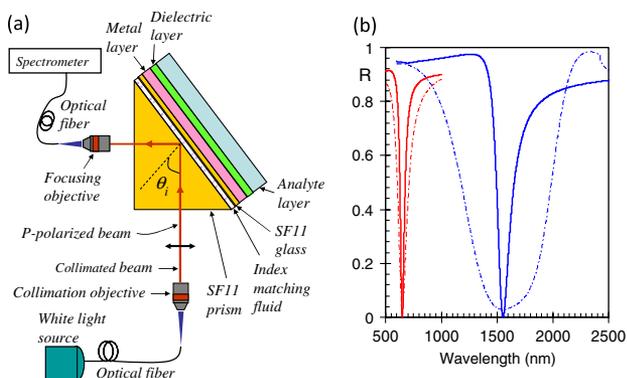
Fig. 1.   (Color online) (a) Schematic illustration of the SPR set-up in the spectral interrogation mode. (b) Spectral reflectivity of SPR (dashed lines) versus NGWSPR (solid lines) in both the visible region and the IR region. In the visible region, the Ag layer thickness is 46 nm for both SPR and NGWSPR, the Si layer thickness is 10 nm, and the incidence angles are 52.3° (for SPR) and 67.3° (for NGWSPR). In the IR region, the Ag and Si layers' thicknesses are 33 and 50 nm, respectively, and the incidence angles are 50.3° for SPR and 58.50° for NGWSPR. For all curves, the prism is SF11 and the analyte RI is 1.33.
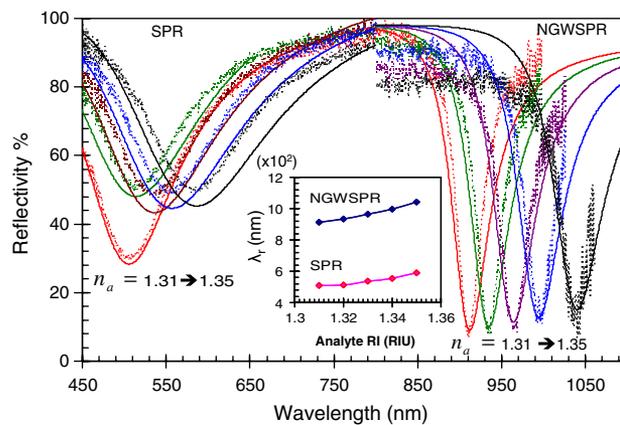

Fig. 2.   (Color online) Reflectivity versus wavelength for the SPR (curves in the left side) and NGWSPR (curves in the right side). The dotted lines correspond to the measurements and the solid lines to the theoretical calculations. For both SPR and NGWSPR, the analyte RI changes from 1.31 to 1.35 (as indicated below each curve) by steps of 0.01. The inset shows the measured resonance wavelength versus the analyte RI for both SPR and NGWSPR.

thicknesses of the Ag and Si layers in the NGWSPR structure were estimated to be 50 and 15.7 nm, respectively, while the Ag and thiol layers' thicknesses in the SPR structure were estimated to be 33 and 5 nm, respectively. The incidence angle in the spectral interrogation mode was set to 54.7° inside the prism. The spectrum of the reflectance for both SPR and NGWSPR structures were recorded when the reflectance in the TE state was taken as a reference signal to the measurements.

As it is known in SPR sensors, all the techniques that are applied to enhance the sensitivity are accompanied by a significant broadening of the dip that characterizes the SPR response in both angular interrogation mode and spectral mode. This broadening deteriorates the resolution of the measurement and consequently harms the low limit of detection (LOD) of the system. Investigating the NGWSPR configuration when the spectral mode is used shows that this trade-off between the sensitivity enhancement and FOM improvement can be resolved. Figure 1(b) clearly demonstrates that adding a thin Si layer above the metallic layer significantly narrows the dip. The comparison between SPR and NGWSPR dip widths was performed by adjusting the incidence angle in order to obtain the resonance in both the visible region ($\lambda_{\mathrm{res}} =$ 650 nm) and the IR range ($\lambda_{\mathrm{res}} =$ 1550 nm). This narrowing ratio can vary from $1:2.33$ in the visible region up to $1:5$ in the IR region. The relatively higher narrowing observed in the IR range is due to the negligible absorption in Si in this region. The broadening in the SPR dip when the resonance wavelength increases is a general feature, which occurs due to the strong absorption of the metal, which considerably increases for longer wavelengths.

In Figure 2, both experimental and theoretical fit curves of the spectral response of the two structures are presented. One can see from Fig. 2 that the shift in the resonance wavelength for the conventional SPR structure was about 80 nm when the analyte RI changed from 1.31 to 1.35, while the shift in the resonance wavelength for the NGWSPR structure was about 130 nm for the

same change in the analyte RI. These values of the shift correspond to the experimental results when the incidence angle was kept fixed. In the theoretical simulations [16], the SF11 prism dispersion was taken into account. The spectral regions in Fig. 2 with high fluctuations are due to the low signal-to-noise ratio (SNR) obtained in the spectrometer in these regions.

Spectral sensitivity scales with λ_{res}, which is determined solely by the incidence angle. This fact was extensively elaborated by Homola [17]. In the SPR structure, increasing λ_{res} is achieved by decreasing the incidence angle, which deteriorates the width of the dip as well. When the incidence angle is similar to both SPR and NGWSPR, the λ_{res} that is obtained in the NGWSPR is significantly larger than its counterpart in the SPR structure. The redshift in λ_{res} due to the Si overlayer not only increases the spectral sensitivity of the sensor but also improves the accuracy of the measurement due the narrowing of the dip.

In order to examine the overall effect of adding the Si overlayer on both the spectral sensitivity and the dip width, the FOM of both SPR and NGWSPR structures was calculated. Figure 3(a) demonstrates that the FOM is improved as well when the NGWSPR structure is used. The behavior of the sensitivity and the dip width were examined and compared for both SPR and NGWSPR at the same incidence angles [Fig. 3(b)]. Because small incidence angles often correspond to the IR region, the advantage of the NGWSPR on the SPR seems to be more prominent at this spectral region. The comparison presented in Fig. 3 was done when the Si layer thickness is fixed. By optimizing the overlayer thickness, in particular in the IR region, the dip width can be further decreased and the FOM can be further improved.

The sensitivity scales with the interaction volume of the EM intensity and the analyte medium, namely the overlap integral on the electromagnetic (EM) intensity inside the analyte region [16]. Theoretical calculations showed that adding the Si overlayer not only enhances
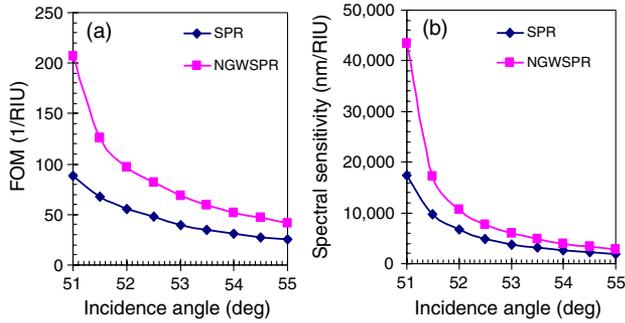
Fig. 3.   (Color online) (a) FOM as a function of the incidence angle for both SPR and NGWSPR. (b) Spectral sensitivity as a function of the incidence angle for both SPR and NGWSPR. An SF11 prism was used, analyte RI $(n_a) = 1.33$, Ag layer thickness was optimized to give full matching condition, and the Si layer thickness is 10 nm. For the same incidence angles range, the resonance wavelength varies from 860 to 530 nm in the SPR case and from 1400 to 820 nm in the NGWSPR case.

the EM fields at the analyte interface, but also increases the penetration depth inside the analyte due to the larger resonance wavelength. These two effects together increase the energy that propagates parallel to the analyte interface and extend the sensing range inside the sample.

Although the spectral dip becomes narrower when the Si overlayer is added, the propagation distance of the surface plasmon (SP) wave parallel to the analyte interface is not larger due to this narrowing as may be expected. To examine this behavior, the dispersion relation of the NGWSPR structure was derived (Eq. 1), from which the SP wave vector $K_{SP} = K'_{SP} + i \cdot K''_{SP}$ can be calculated:

$$\exp(-2k_{zm} \cdot d_m) = -[r_{ms} \cdot r_{sa} \cdot \exp(-2k_{zs} \cdot d_s) + 1]$$
$$/[r_{pm} \cdot r_{sa} \cdot \exp(-2k_{zs} \cdot d_s) + r_{pm} \cdot r_{ms}]$$
$$r_{ij} = \left(\frac{k_{zi}}{\varepsilon_i} - \frac{k_{zj}}{\varepsilon_j}\right) \bigg/ \left(\frac{k_{zi}}{\varepsilon_i} + \frac{k_{zj}}{\varepsilon_j}\right);$$
$$k_{zi} = \sqrt{\varepsilon_i k_0^2 - k_{SP}^2}. \tag{1}$$

Here $i, j = p, m, s, a$ refer to the prism, metal, silicon, and analyte, respectively; k_{zi} and ε_i are the z component of the K vector and the permittivity of medium (i), respectively; and d_m and d_s are the thicknesses of the metal and the silicon layers, respectively. Solving the dispersion relation [Eq. (1)] yields that the imaginary part of the SP K-vector increases with adding the Si layer, although

the dip is narrower. This shows that the spectral dip width has a complicated dependence on the metal and the prism dispersion different from the angular dip width behavior, which is proportional to the reciprocal of K''_{SP}.

To conclude, the spectral sensitivity and FOM of SPR sensors can be enhanced significantly by introducing a thin dielectric overlayer in the KR configuration. Adding this nanodimensional thin film with high RI not only enhances the sensitivity of the sensor but also improves the resolution of the measurement, increases the FOM, and improves the stability of the sensor.

References

1. A. Shalabney and I. Abdulhalim, Laser Photon. Rev. **5**, 571 (2011).
2. G. Gupta and J. Kondoh, Sensors Actuators B **122**, 381 (2007).
3. J. S. Yuk, D. Hong, J. Jung, S. Jung, H. Kim, J. Han, Y. Kim, and K. Ha, Eur. Biophys. J. **35**, 469 (2006).
4. X. Yuan, B. H. Ong, Y. G. Tan, D. W. Zhang, R. Irawan, and S. C. Tjin, J. Opt. A **8**, 959 (2006).
5. A. Shalabney, A. Lakhtakia, I. Abdulhalim, A. Lahav, C. Patzig, I. Hazek, A. Karabchevsky, B. Rauschenbach, F. Zhang, and J. Xu, Photon. Nanostruct. Fundam. Appl. **7**, 176 (2009).
6. A. Shalabney, C. Khare, B. Rauschenbach, and I. Abdulhalim, Sensors Actuators B **159**, 201 (2011).
7. S. Y. Wu, H. P. Ho, W. C. Law, C. Lin, and S. K. Kong, Opt. Lett. **29**, 2378 (2004).
8. V. Kabashin and P. I. Nikitin, Opt. Commun. **150**, 5 (1998).
9. H. Suzuki, M. Sugimoto, Y. Matsui, and J. Kondoh, Meas. Sci. Technol. **17**, 1547 (2006).
10. A. Lahav, M. Auslender, and I. Abdulhalim, Opt. Lett. **33**, 2539 (2008).
11. A. Lahav, A. Shalabaney, and I. Abdulhalim, J. Nanophoton. **3**, 031501 (2009).
12. Z. Salamon, H. A. Macleod, and G. Tollin, Biophys. J. **73**, 2791 (1997).
13. T. H. Gilani, N. Dushkina, W. L. Freeman, M. Z. Numan, D. N. Talwar, and D. P. Pulsifer, Opt. Eng. **49**, 120503 (2010).
14. V. Yashunsky, V. Lirtsman, M. Golosovsky, D. Davidov, and B. Aroeti, Biophys. J. **99**, 4028 (2010).
15. P. Bhatia and B. D. Gupta, Appl. Opt. **50**, 2032 (2011).
16. A. Shalabney and I. Abdulhalim, Sensors Actuators A **159**, 24 (2010).
17. J. Homola, Sensors Actuators B **41**, 207 (1997).